Electronic Supplementary Material (ESI) for Chemical Science.

Metabolic mechanisms of a drug revealed by distortion-free ^{13}C tracer analysis

Jin Wook Cha,[a‡] Xing Jin,[b‡] Sihyang Jo,[b] Yong Jin An[b*] and Sunghyouk Park[b*]

[a] Natural Product Informatics Research Center, KIST Gangneung Institute of Natural Products, Gangneung, 25451, Korea

[b] Natural Product Research Institute, College of Pharmacy, Seoul National University, 1 Gwanak-ro, Gwanak-gu, Seoul 08826, Korea

[‡] These authors contributed equally to this work

* **Author to whom all correspondence should be addressed.**

Yong Jin An

Address) College of Pharmacy, Seoul National University, 1 Gwanak-ro, Gwanak-gu, Seoul 08826, Korea

E-mail) biochem.yong@gmail.com

Phone) +82-2-880-7831

Fax) +82-2-880-0649

Sunghyouk Park:

Address) College of Pharmacy, Seoul National University, 1 Gwanak-ro, Gwanak-gu, Seoul 08826, Korea

E-mail) psh@snu.ac.kr

Phone) +82-2-880-7831

Fax) +82-2-880-0649

Materials and Methods

- Chemicals and reagents

Stable isotopes were purchased from Cambridge isotope laboratories (Tewksbury, MA, U.S.A.). These include Glucose (U-$^{13}C_6$, 99%), L-Glutamine ($^{13}C_5$, 99%, $^{15}N_2$, 99%), Alpha-ketoglutaric acid ($^{13}C_5$, 99%), Alpha-ketoglutaric acid (1,2,3,4-$^{13}C_4$, 99%), and Sodium L-lactate ($^{13}C_3$, 98%).

- Cell line and culture condition

The mouse lymphocytic leukemia L1210 cells were purchased from American Type Culture Collection (ATCC). Cells were cultured in high glucose (25 mM) DMEM medium (Welgene, Daegu, Korea) supplemented with 10% fetal bovine serum (FBS, Welgene, Daegu, Korea) and 1% penicillin−streptomycin solution (Gibco, Grand Island, NY). The Cells were cultured at 37 ^{o}C in a 5% CO_2 humidified incubator.

- Stable isotope labeling

L1210 cells (5 x 10^8) were washed with DPBS and resuspended with 30 mL of glucose, pyruvate-free DMEM media (Gibco, Waltham, MA) supplemented with 10% dialyzed FBS (Gibco, Waltham, MA), 1% penicillin-streptomycin (Gibco, Waltham, MA), and 25 mM U-$^{13}C_6$ glucose. For the dichloroacetate (DCA, Sigma-Aldrich, St Louis, MO) treatment, final 10 mM DCA was added to the media and the cells were incubated at 37 ^{o}C in a 5% CO_2 incubator for overnight.

- Extraction and NMR and MS sample preparation

Stable isotope labeled L1210 cells were washed twice with cold DPBS by centrifugation. Methanol (400 µL) and chloroform (200 µL) were added. Then, the following procedure was repeated three times; vortexing for 30 seconds, snap-freezing in liquid nitrogen (1min), and thawing (2 min) on ice. Additional 200 µL of chloroform and 200 µL of distilled water were added and the sample was vortexed for 30 sec. Then the sample was centrifuged at 15,800 g for 20 min at 4 ^{o}C. After centrifugation, the aqueous layer and lipid layer were carefully transferred into a new microcentrifuge tube. The samples were aliquotted for NMR (90%) and MS (10%) analysis and dried using SpeedVac (Vision, Gyeonggi-do, Korea). The dried samples were stored -20 ^{o}C until measurements.

- NMR measurement and data processing

The dried samples were dissolved in 500 µL of NMR buffer (2 mM Na_2HPO_4, 5 mM NaH_2PO_4, 0.025% TSP in D_2O). The data were obtained with an 800 MHz Bruker Avance III HD spectrometer equipped with a 5 mm CPTCI CryoProbe (College of pharmacy, Seoul National University, Seoul, Korea) and 850 MHz Bruker Avance III HD spectrometer equipped with a CryoProbe (National Center for Inter-University Research Facilities, Seoul National University, Seoul, Korea). HSQC NMR spectra were acquired with the following parameters: pulse program, 'hsqcetgpsisp2.2' and the one in ***Figure S2***; acquisition time, ~ 11 min; spectral widths, 16 ppm (^{1}H) and 40 ppm (^{13}C); Frequency offsets, 4.7 ppm (^{1}H) and 27 ppm (^{13}C); time points, 2048 (t_2)×150 (t_1) complex points; Number of scans, 2. For non-uniform sampling (NUS), sampling density were set as follows: 25% of 600 (t_1) complex points. For apodization, cosine-squared function was employed and zero-filling was applied to both dimensions. For the distortion free approach, the indirect frequency domain was reversed in the processing step.

For the isotopomer analysis of glutamate, C4 doublet and quartet volumes were used. The C4 signal is the best probe for the TCA-cycle, as the two-carbon unit from acetyl CoA is incorporated to the C4 and C5 of glutamate, making it a direct reporter for new TCA cycle turns driven by the acetyl CoA incorporation. In addition, its doublet and quartet exhibit simultaneous decrease and increase with the TCA-cycle progression, respectively. This makes the double/quartet ratio very sensitive to the TCA-cycle turns. For the C2, its singlet and doublet intensities do not change. For the C3, the singlet, doublet and triplet are observed, instead of a quartet, because J_{23} (34.8 Hz) and J_{34} (34.5 Hz) are essentially the same. However, the changes in the doublet and triplet are almost parallel, and their ratio is uniform. These behaviors of C2 and C3 multiplets make their use impractical for the isotopomer analysis.

- LC-MS-based isotope enrichment analysis

The dried samples were dissolved in 75 µL of DW: acetonitrile (ACN) (1:1 v/v) and centrifuged at 14,000 g at 4°C for 5 min and a total of 3 µL was injected. Metabolites were separated using a SeQuant® ZIC-HILIC 3.5 µm, 200 Å 100 x 2.1 mm at 30 °C using Vanquish™ UPLC (Thermo Fisher Scientific, Waltham, MA) coupled with Q Exactive™ Plus Hybrid Quadrupole-Orbitrap™ Mass Spectrometer (Thermo Fisher Scientific, Waltham, MA). The mobile phases were 10 mM ammonium acetate in 100% DW (A) and 10 mM ammonium acetate in DW:ACN (1:3) (B) with the gradient as follows: 0 % A at 0 min, 0 % A at 1 min, 80 % A at 7 min, 80 % A at 11 min, 0 % A from 11.1 to 23 min with a 0.4 mL/min flow rate. The Q Exactive Plus MS system was equipped with a Heated electrospray ionization (HESI-II) probe with the following settings: sheath gas = 50 mL/min; auxiliary gas = 15 mL/min, heated to 350 °C; sweep gas = 2 mL/min; spray voltage = 2.5 kV, capillary temperature = 320°C; S-lens RF level = 50. Metabolites were detected in negative polarity. Isotopologue peaks were extracted using Xcalibur ver. 2.8 (Thermo Fisher Scientific, Waltham, MA).

Figure S1. Origin of the phase distortion during the coherence selection period due to the J_{CC} coupling interaction.

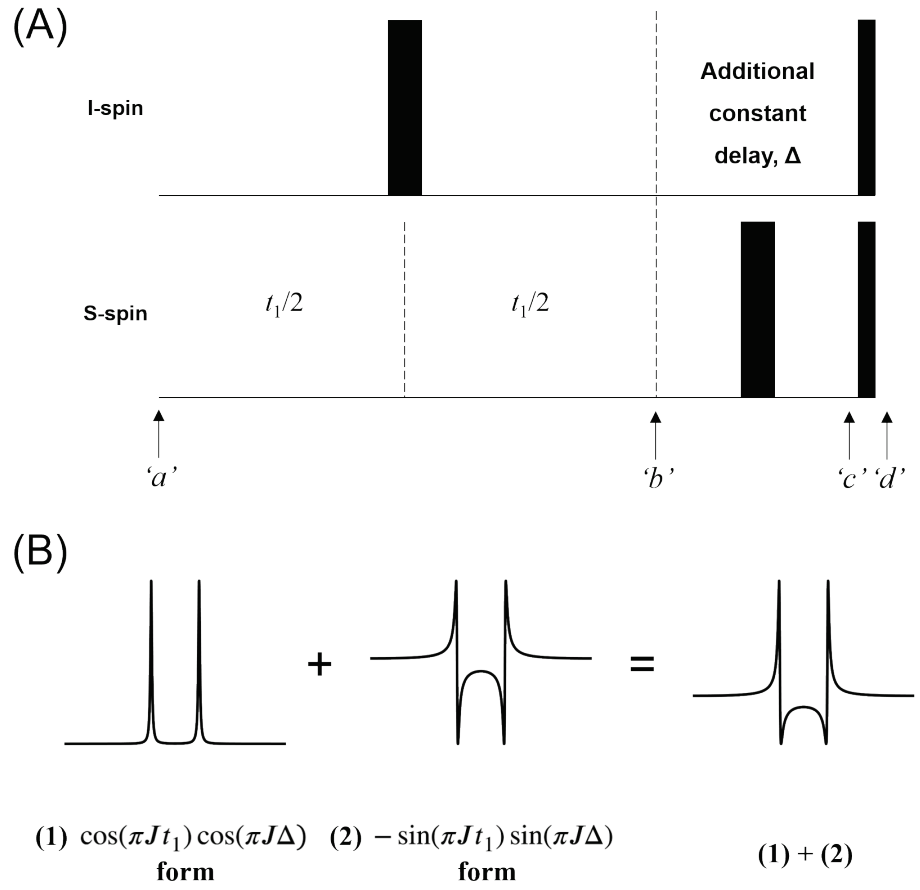

(A) The t_1-evolution period and an additional constant delay (i.e. for gradient selection), Δ, for coherence selection in a typical gradient-selected HSQC experiment. All pulses are of phase, *x*. (B) Phase-distorted signals at '*d*' in (A) due to the coexistence of cosine and sine *J*-modulated terms in t_1. (see below for product operator analysis)

signals for the *S* spin. Without the additional constant delay, Δ, only the cosine *J*-modulated signals would remain, and pure absorptive signals could be obtained. The detailed product operator analysis is given below.

As described in the main text, the constant interval after the t_1-evolution period can give rise to a phase distortion due to the survival of both cosine and sine J-coupling modulation terms during t_1.

Assume that the product operator at a point '*a*' in the supplementary figure 1 has the form of

$$-2\hat{S}_{1y}\hat{I}_z$$

with the Hamiltonian $\hat{H}_0 = \Omega_1\hat{S}_{1z} + 2\pi J_{12}\hat{S}_{1z}\hat{S}_{2z} + 2\pi J_{IS_1}\hat{I}_z\hat{S}_{1z}$ where I and S spins denote ^{1}H and ^{13}C spin, respectively. Ω_1 is the chemical shift of $\hat{S}_1$. J_{12} and J_{IS_1} are the scalar coupling constants between spins in the subscripts.

At a point '*b*' the product operator can be expressed as

$$-2\hat{S}_{1y}\hat{I}_z \xrightarrow{\Omega_1\hat{S}_{1z}t_1+2\pi J_{12}\hat{S}_{1z}\hat{S}_{2z}t_1+2\pi J_{IS_1}\hat{I}_z\hat{S}_{1z}t_1} \xrightarrow{\pi\hat{I}_x} +2\hat{I}_z\{\hat{S}_{1y}\cos(\Omega_1 t_1)\cos(\pi J_{12}t_1) - 2\hat{S}_{1x}\hat{S}_{2z}\cos(\Omega_1 t_1)\sin(\pi J_{12}t_1) - \hat{S}_{1x}\sin(\Omega_1 t_1)\cos(\pi J_{12}t_1) - 2\hat{S}_{1y}\hat{S}_{2z}\sin(\Omega_1 t_1)\sin(\pi J_{12}t_1)\}$$

Among those, without the additional delay, Δ, the only finally observable term after the mixing and reverse INEPT in HSQC would be

$$2\hat{I}_z\hat{S}_{1y}\cos(\Omega_1 t_1)\cos(\pi J_{12}t_1)$$

As a routine HSQC experiment has the additional delay for gradient coherence selection, the ^{13}C-^{13}C homonuclear J-coupling for uniformly ^{13}C-labeled tracers during the period can further convert the J-coupling anti-phase operator to an in-phase form for the ***S*** spin and *vice versa* at a point '*c*', as follows.

$$2\hat{I}_z \cos(\Omega_1 t_1)\cos(\pi J_{12} t_1)\{\hat{S}_{1y}\} \xrightarrow{2\pi J_{12}\hat{S}_{1z}\hat{S}_{2z}\Delta} -2\hat{I}_z \cos(\Omega_1 t_1)\cos(\pi J_{12} t_1)\{\hat{S}_{1y}\cos(\pi J_{12}\Delta) - 2\hat{S}_{1x}\hat{S}_{2z}\sin(\pi J_{12}\Delta)\} \quad \text{(A)}$$

$$-2\hat{I}_z \cos(\Omega_1 t_1)\sin(\pi J_{12} t_1)\{2\hat{S}_{1x}\hat{S}_{2z}\} \xrightarrow{\pi\hat{S}_x} 2\hat{I}_z \cos(\Omega_1 t_1)\sin(\pi J_{12} t_1)\{2\hat{S}_{1x}\hat{S}_{2z}\cos(\pi J_{12}\Delta) + \hat{S}_{1y}\sin(\pi J_{12}\Delta)\} \quad \text{(B)}$$

Thus, the first term of the right-side in equation (A) and second term of the right-side equation (B) can be attributed to observable signals. Since the second term in (B) has sine modulated J-coupling term in t_1, the final form of observable product operators after mixing pulse at a point '*d*', is expressed as by a combination of cosine and sine modulated J-coupling terms in t_1.

$$2\hat{I}_y\hat{S}_{1z}\cos(\Omega_1 t_1)\{\cos(\pi J_{12} t_1)\cos(\pi J_{12}\Delta) - \sin(\pi J_{12} t_1)\sin(\pi J_{12}\Delta)\}$$

Figure S2. Proposed pulse sequence of *J*-scaled distortion-free HSQC.

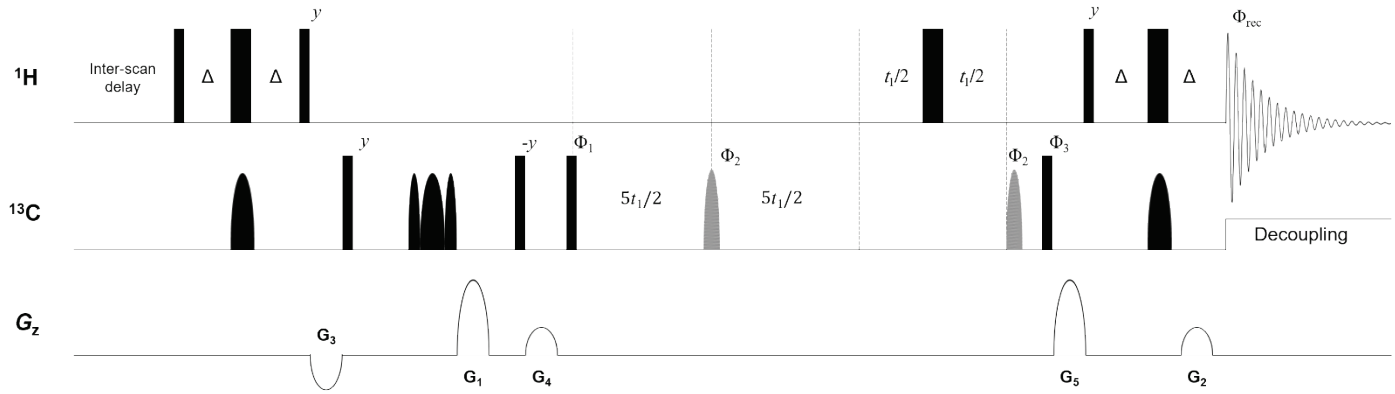

Proposed pulse sequence of J-scaled distortion-free HSQC. Narrow and wide bars represent 90° and 180° hard pulses, respectively. Black semi-ellipse boxes indicate adiabatic inversion (single semi-ellipse box; Crp80,0.5.,20.1) and refocusing (composite semi-ellipse boxes; Crp80comp.4) pulses, respectively. For a detailed adiabatic pulse parameter, *see **Table S2***. Gray semi-ellipse boxes indicate short adiabatic inversion pulses (Tanh/Tan; *see parameter topic*). The inter-scan delay was 1 s and the delay Δ was set to $1/4J_{CH}$=1.72 ms. All pulses are of phase, *x,* unless otherwise indicated. For the phase-sensitive acquisition in the indirect domain, STATES-TPPI detection mode was employed. The phase cycling is as follows. Φ_1 = *x*, -*x*; Φ2 = -*y*, -*y*, *y*, *y*; Φ_3 = -*x*, -*x*, *x*, *x* Φ_{rec} = *x*, -*x*, -*x*, *x*. Gradient ratios: G_1 : G_2 = 4 : 1 and G_3, G_4 and G_5 are homospoil gradient pulses. Decoupling is achieved with bilevel decoupling sequence (bi_p5m4sp_4sp.2).

As the interval for frequency discrimination in a gradient-selected HSQC [1] causes phase distortions, we employed STATE-TPPI [2] frequency discrimination which does not require an additional delay. Still, to suppress possibly deleterious t_1-noise from strong signals and to observe weak signals from complex cell extracts [3], it was necessary to keep the gradient selection scheme. Therefore, we moved the PFG spin-echo element from the t_1-evolution period and placed it before the t_1-evolution period. In addition, as a conventional adiabatic refocusing pulse has a considerable pulse length that can also cause non-negligible J-coupling evolution, we employed a short adiabatic inversion pulse. To avoid possible phase errors associated with adiabatic refocusing pulses [4], we employed a pair of short adiabatic inversion pulses [5]. The pulse scheme features a six-fold J-scaled distortion-free HSQC pulse sequence.

Figure S3. Analytical simulation of the new experiment described in the Figure S2.

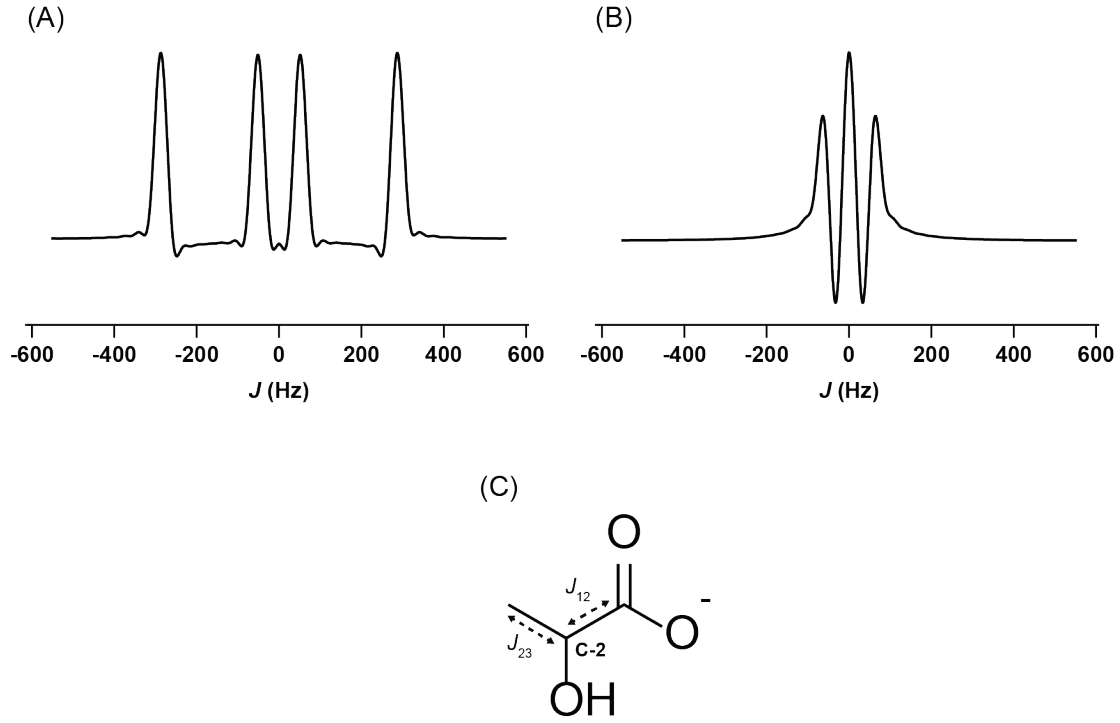

Comparison of simulated 1D F_1-projected J-scaled distortion-free and conventional HSQC spectra for the C2 carbon of U-$^{13}C_3$-lactate. (A) A simulated F_1-projected J-scaled distortion-free HSQC with scaling factor six. (B) A simulated 1D F_1-projected sensitivity enhanced (PEP)-HSQC spectrum. (C) The structure of U-^{13}C lactate; J_{ab} indicates homonuclear J-coupling constant between ^{13}C spin C-*a* and C-*b* position. For the simulation, ^{13}C-^{13}C *J*-coupling constants were set to J_{12} J_{12} = 56 Hz and J_{23} = 39 Hz. For a detailed simulation parameter, *see below*.

A simulation of 1D projection HSQC spectra was plotted by home-built python 3.6 script. A signal plotting was carried out according to an equation (1) where an $L-1$ is the number of spins that are weakly coupled with spin S_1, and J_k is the *J*-coupling constant between ^{13}C spins S_1 and S_k. R_2 , the spin-spin relaxation rate constant, was set to 1 (Here, for brevity, the spin relaxation outside the t_1-evolution period was neglected). For a simulation of conventional PFG-PEP-HSQC type spectrum (hsqcetgpsisp2.2), additional constant delay Δ and scaling factor (N) were set to 4.4 ms and 1, respectively. For the simulation of J-scaled distortion-free HSQC type spectrum, additional constant delay Δ and scaling factor (N) were set to 600 μs and 6, respectively. For the Fourier transformation, f_{max} was set to 550 Hz and time-domain points to 33 points with the final 4096 points after zero-filling. For the apodization, the cosine-squared function was employed.

$$S(t_1) \propto \left[\prod_{k=2}^{L}\{\cos(\pi \mathrm{N} J_k t_1)\cos(\pi \mathrm{N} J_k \Delta) - \sin(\pi \mathrm{N} J_k t_1)\sin(\pi \mathrm{N} J_k \Delta)\}\right] \cdot \exp(-R_2 t_1) \qquad (1)^*$$

---

* In a more explicit expression of the signal form of the PFG-PEP-HSQC with $I_n S$ spin system, i.e., CH_n, the signal function (eq. (1)) is multiplied by an additional term "$\sqrt{2}\cos(\pi J_{1k}\Delta_2)\cdot\cos^{n-1}(\pi J_{IS}\Delta_2)$", where Δ_2 is the length of the first reverse INEPT sequence and J_{IS} is heteronuclear J-coupling constant between I and S spin. Here, the factor $\sqrt{2}$ is for the theoretical sensitivity-enhancement of PEP sequence. However, the additional term was not used since it does not affect the entire signal form.

Figure S4. Relative isotopologue abundance of acetyl-CoA.

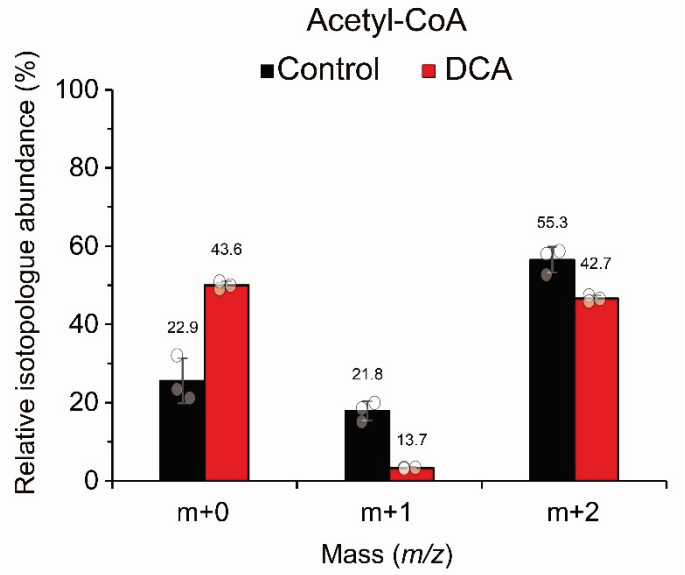

Relative isotopologue abundance of acetyl-CoA from L1210 treated with 25 mM U-$^{13}C_6$-glucose and 10 mM DCA, observed by mass spectrometry. Relative abundance was obtained by normalizing each intensity against the sum of the total intensities.

Figure S5. ^{13}C-^{13}C *J*-coupling patterns for C3 of lactate

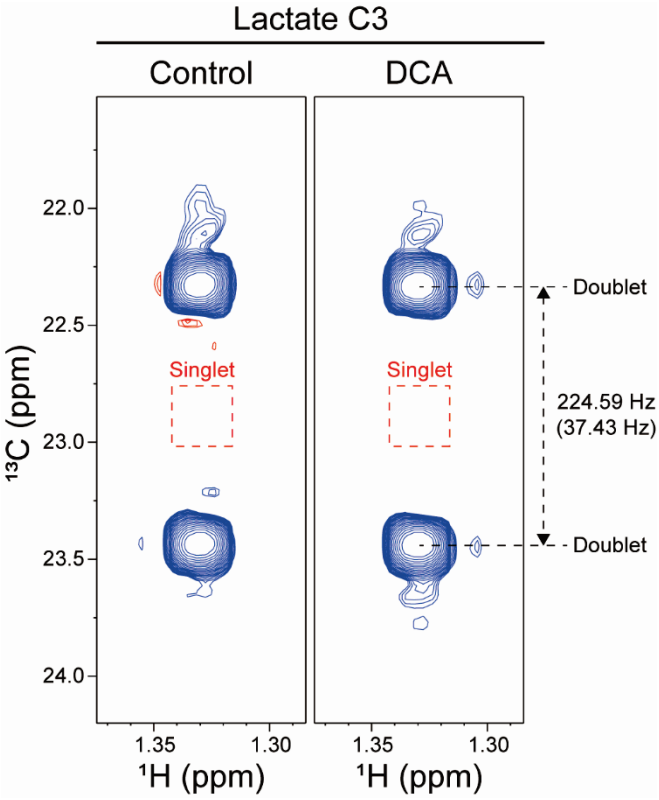

Comparison of spectra for C3 of lactate from L1210 cell extracts with DCA obtained with 6-fold *J*-scaled distortion-free HSQC.

Figure S6. Carbon shuffling through PPP and the resulting isotopomers of serine.

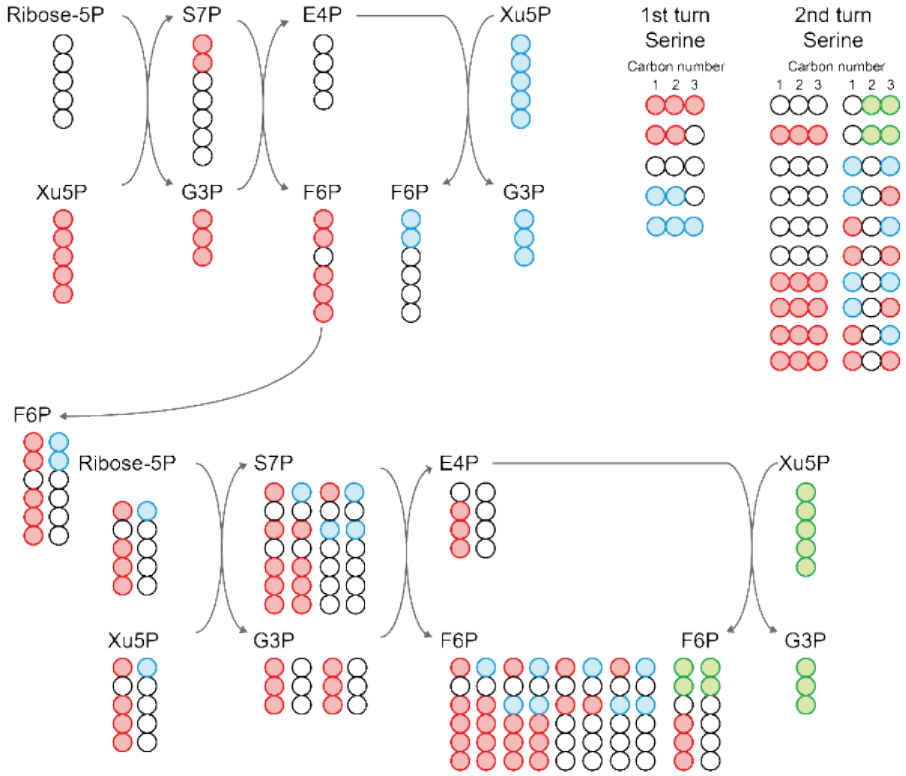

Carbon shuffling as U-$^{13}C_6$-glucose is metabolized through PPP, and the resulting serine labeling patterns. Each color fill represents ^{13}C-carbon introduced from a different molecule.

Table S1. Comparison of the multiplet quantitation by NUS and *J*-scaling

Absolute volume: Volume × 10^6

Method	***J*-scaling**						**NUS**					
Isotopomer type	1,2,3,4-$^{13}C_4$-αKG		U-$^{13}C_5$-αKG				1,2,3,4-$^{13}C_4$-αKG		U-$^{13}C_5$-αKG			
Multiplet type	D_1	D_2	Q_1	Q_2	Q_3	Q_4	D_1	D_2	Q_1	Q_2	Q_3	Q_4
Abs.	30.847	33.563	17.246	16.866	14.962	18.221	51.615	49.812	28.795	24.980	55.502	34.440
Rel.	1	1.088	1.023	1	0.887	1.080	1.036	1	1.15	1	2.223	1.379
Abs.	64.410		67.295				101.427		143.717			
Rel.	1		1.045				1		1.417			

The peaklets within each C4 multiplet (D or Q) from the 1:1 mixture of 1,2,3,4-$^{13}C_4$ αKG and U-$^{13}C_5$ αKG were quantified by their volume in spectra (Figure 3) obtained using each method. D = doublet, Q = quartet. Abs. = Absolute volume, Rel. = Relative volume.

Table S2. Parameters for the adiabatic pulses employed in the *J*-scaled distortion-free HSQC pulse sequence.

Pulse	Duration (μs)	$\gamma B_{1,max}$ (Hz)	Sweep width (kHz)
Tanh/Tan, *R* = 390	300	14051	1300
[a]Crp80comp.4	2000	11283	80
[b]Crp80,0.5,20.1	500	11283	80

[a,b] From Topspin 3.6 preset adiabatic pulses

Reference

[1] A. L. Davis, J. Keeler, E. D. Laue, D. Moskau, *J. Magn. Reson.* **1992**, *98*, 207-216.
[2] D. Marion, M. Ikura, R. Tschudin, A. Bax, *J. Magn. Reson.* **1989**, *85*, 393-399.
[3] A. F. Mehlkopf, D. Korbee, T. A. Tiggelman, R. Freeman, *J. Magn. Reson.* **1984**, *58*, 315-323.
[4] T. L. Hwang, P. C. Van Zijl, M. Garwood, *J. Magn. Reson.* **1997**, *124*, 250.
[5] T. L. Hwang, A. Shaka, *J. Magn. Reson., Ser. A* **1995**, *112*, 275-279.